

Exchange coupling in transition metal monoxides

Guntram Fischer,¹ Markus Dane,^{2,3} Arthur Ernst,² Patrick Bruno,^{2,4} Martin
Luders,⁵ Zdzisław Szotek,⁵ Walter Tilmann,⁵ and Wolfram Hergert¹

¹Institute of Physics, Martin Luther University Halle-Wittenberg,
Von-Seckendorff-Platz 1, D-06120 Halle, Germany

²Max Planck Institute of Microstructure Physics, Weinberg 2, D-06120 Halle, Germany

³ORNL, P.O. BOX 2008 MS6114, Oak Ridge TN 37831-6114, USA

⁴European Synchrotron Radiation Facility, BP 220, F-38043 Grenoble Cedex, France

⁵Daresbury Laboratory, Daresbury, Warrington, WA4 4AD, UK

(Dated: February 21, 2024)

An *ab initio* study of magnetic exchange interactions in antiferromagnetic and strongly correlated 3d transition metal monoxides is presented. Their electronic structure is calculated using the local self-interaction correction approach, implemented within the Korringa-Kohn-Rostoker band structure method, which is based on multiple scattering theory. The Heisenberg exchange constants are evaluated with the magnetic force theorem. Based on these the corresponding Neel temperatures T_N and spin wave dispersions are calculated. The Neel temperatures are obtained using mean field approximation, random phase approximation and Monte Carlo simulations. The pressure dependence of T_N is investigated using exchange constants calculated for different lattice constants. All the calculated results are compared to experimental data.

I. INTRODUCTION

In the last years there has been a general strong interest in finding materials with specific or even paramagnetic properties. Such materials could be useful in the field of spintronics. A lot of the promising candidates are strongly correlated electronic systems which in many ways are still a challenge to be properly described theoretically regarding their electronic ground state properties. On the other hand, for reliable predictions about magnetic properties of materials it is essential to have theories describing the magnetism adequately by quantitative and qualitative means. One of these theories is the Heisenberg theory of magnetism, which we shall apply in the present paper. Its central quantities are the Heisenberg exchange constants J_{ij} , which are of general fundamental interest. In particular they provide information about the magnetic periodicity (via their Fourier transform), the spin-wave dispersion, magnetic critical temperatures and also allow predictions on structural effects caused by magnetism^{1,2}.

In this paper we concentrate on the study of the magnetic exchange interactions of transition metal monoxides (TMOs), specifically MnO, FeO, CoO and NiO. They are charge-transfer insulators, well known for strong correlation effects associated with the TM 3d-electrons. Originating from the Anderson-type superexchange, their equilibrium magnetic structures are of the antiferromagnetic II (AF II) order, characterized by planes of opposite magnetization which are stacked in (111)-direction. Recently, a Mott transition has been observed in MnO at high pressure of about 105 GPa, in resistivity³ and X-ray spectroscopy measurements^{4,5} which stimulated new theoretical studies in this high pressure region.^{6,7} There already exists a large body of neutron scattering measurements of magnetic structures and magnetic excitations in transition metal monoxides. However, the development

of new experimental techniques such as neutron powder diffraction^{8,9,10} and polarized neutron reflectivity¹¹ has renewed interest in studying TMOs as antiferromagnetic benchmark materials. Modern neutron spectrometers operate with such a high efficiency that also high angle diffraction experiments can be performed to unravel complex magnetic order e.g. in thin films¹².

From the theory point of view conventional methods such as the local spin density approximation (LSDA) to density functional theory (DFT), treating electron correlations at the level of the homogeneous electron gas, fail to provide an adequate description of the electronic structure of these oxides. Over the years a number of approaches has been developed, aiming at improvements to the LSDA treatment of electron correlations, and applied to TMOs with varying degrees of success. Among them are: the LSDA + U method^{13,14}, GGA + U¹⁵, self-interaction corrected (SIC)-LSDA^{16,17,18,19,20,21}, hybrid functionals^{22,23}, and finally dynamical mean field theory²⁴. In general, they have improved lattice constants, band gaps and magnetic properties, some of them have also obtained good agreement with spectroscopies. In the present paper we shall use the so-called local self-interaction correction²⁵ (LSIC) scheme for the calculation of the electronic ground states of the TMOs. As the aim is the investigation of magnetic interactions we combine the LSIC scheme with the magnetic force theorem (MFT)²⁶ in order to obtain the Heisenberg exchange parameters J_{ij} .

The LSIC scheme²⁷ is based on the implementation of the SIC-LSDA formalism^{16,17,25} within multiple scattering theory in the framework of the Korringa-Kohn-Rostoker (KKR) band structure method. It was first applied to f-electron systems^{27,28}, but recently also to TMOs²¹. Within the KKR method one calculates the Green function of the investigated system. This Green function is then straightforwardly used in the application of the

MFT. It is for the first time that this combined approach is applied for calculating exchange constants of the transition metal monoxides. The results of that are compared to the exchange constants extracted from the total energy differences for a number of magnetic structures and mapping them onto a Heisenberg Hamiltonian. Most of the earlier applications of the latter approach have been based on the assumption that only the first two exchange interaction constants are nonzero. Although the present combined approach also relies on the mapping onto a Heisenberg Hamiltonian the assumptions regarding the number of non-zero exchange constants are not needed, which is advantageous to systems with reduced symmetry such as thin films and layered structures (where the justification for such an assumption is not clear from the very beginning).

Having calculated the J_{ij} for the ground states of the TMOs we also calculate and discuss them as a function of external pressure for moderate values of the latter. This is mainly inspired by the recent high pressure measurements of TMOs^{3,4,5}.

Based on the calculated magnetic exchange interactions the transition temperatures can be obtained. In this paper it is done in three different ways, namely by applying mean-field approximation (MFA), random phase approximation (RPA), and using classical Monte Carlo (MC) simulations. The respective results are then compared to those obtained from the disordered local moments (DLM) method²⁹, which does not involve mapping onto a Heisenberg Hamiltonian, but is based on the same ground state electronic structure calculations as the present paper²¹. The last subject we focus on are magnetic excitations. On one hand, with given J_{ij} , one can calculate the magnon spectrum of any material. On the other hand, measuring the latter experimentally is a direct method to examine its exchange constants. Thus, comparing calculated to experimental spin wave dispersions provides a straightforward tool for determining the accuracy of the calculated J_{ij} .

The present paper is organized as follows: In section II the theoretical approaches for the calculation of electronic structure, exchange interactions and Neel temperatures are presented. The computational details are described in section III. Section IV contains the results and discussion. The exchange parameters and the Neel temperatures are presented for theoretical equilibrium lattice constants and as a function of lattice constants and pressure, respectively. Finally, the calculated magnon spectra of the TMOs are discussed in reference to experiments. The paper is concluded in section V.

II. THEORY

A. Electronic Structure

For the electronic structure calculations of TMOs we use a multiple scattering theory-based implementation of

the SIC-LSDA method²⁵, whose total energy functional is

$$E^{\text{SIC-LSDA}}[n, g] = E_X^{\text{LSDA}}[n, n_{\#}] + E_H[n] + E_{xc}^{\text{LSDA}}[n, 0]; \quad (1)$$

with the LSDA energy functional in units of Rydberg given by

$$E^{\text{LSDA}}[n, n_{\#}] = \sum_{\mathbf{r}} \sum_{\mathbf{r}'} \sum_{\mathbf{r}''} h_{\mathbf{r}\mathbf{r}'}^2 j_{\mathbf{r}\mathbf{r}'} + E_{\text{ext}} + E_H[n] + E_{xc}^{\text{LSDA}}[n, n_{\#}]; \quad (2)$$

Here $\phi_{\mathbf{r}}$ is a Kohn-Sham orbital, α a multi-index labelling the orbitals and spin (" or #"), respectively, $n = \sum_{\mathbf{r}} \phi_{\mathbf{r}}^2$, $n_{\#} = \sum_{\mathbf{r}} \phi_{\mathbf{r}\#}^2$ and $n = n + n_{\#}$. E_X^{LSDA} differs from E^{LSDA} since the kinetic energy is evaluated with respect to the orbitals minimizing the SIC-functional. The summations run over all the occupied orbitals, E_{ext} denotes the external energy functional due to ion cores, E_H is the Hartree energy and E_{xc}^{LSDA} is the LSDA exchange-correlation energy functional. The second term in Eq. (1) is the so-called self-interaction correction²⁵ for all the occupied orbitals. It restores the property

$$E_H[n] + E_{xc}^{\text{exact}}[n, 0] = 0; \quad (3)$$

that the exact DFT exchange-correlation functional has, namely that for any single orbital density the Hartree term should be cancelled by the corresponding exchange-correlation term. The cost paid for restoring the above property is the orbital dependence of the SIC-LSDA energy functional (Eq. (1)). The correction is only substantial for localized orbital states, but vanishes for itinerant states. In the limit of all itinerant states the SIC-LSDA total energy functional is identically equal to the LSDA functional.

The main idea behind the "local" implementation of the SIC-LSDA formalism (LSIC) is that within multiple scattering theory, in the framework of the KKR method, one works with the scattering phase shifts, describing scattering properties of single atoms in a solid. Among them only the resonant phase shifts are relevant, as they refer to localized states. Thus the self-interaction correction is associated with the on-site scattering potentials and leads to modified resonant scattering phase shifts. In particular, they become stronger localized. Details of the LSIC implementation are discussed in Ref. 27.

B. Magnetic Interactions

The Heisenberg theory of magnetism assumes that it is possible to map magnetic interactions in a material onto localized spin moments, which in a classical picture can be represented by a vector. The resulting classical Hamiltonian,

$$H = \sum_{ij} J_{ij} \mathbf{e}_i \cdot \mathbf{e}_j; \quad (4)$$

contains only the unit vectors $\mathbf{e}_{i(j)}$ of the spin moments and the exchange parameters J_{ij} describing the interactions between them³⁰. Here i and j index the sites.

It should be mentioned here that the Hamiltonian (4) can be extended to include additional effects like magnetocrystalline anisotropy or tetragonal or rhombohedral distortions of the lattice. The latter reflect magnetoelectric effects which result in two different values for the nearest neighbour (NN) exchange parameters, depending on a parallel or antiparallel alignment of the moments. Such effects are usually present in experiments. Thus, special care is required when comparing theoretical and experimental results.

Our method of choice for the calculation of the exchange parameters J_{ij} makes use of the magnetic force theorem, but invokes also mapping onto a Heisenberg Hamiltonian. For comparison, we also apply the most commonly used approach which relies on the calculation of total energy differences between different magnetic configurations and mapping them onto a classical Heisenberg Hamiltonian.

1. Magnetic Force Theorem Approach

The idea behind the magnetic force theorem²⁶ is to consider infinitesimally small rotations of classical spins at two different lattice sites. These give rise to energy changes that are mapped onto the classical Heisenberg Hamiltonian via multiple scattering theory. This approach is based on the assumption that the potentials are unchanged by the rotations. The advantage of the MFT method is that the exchange integrals can be calculated directly in the relevant magnetic structure. The result for the exchange parameter J_{ij} of the two magnetic moments at sites i and j can be written as

$$J_{ij} = \frac{1}{8} \sum_{\mathbf{r}} \text{Tr} \left[\hat{U}_{i\mathbf{r}}^{\dagger} \hat{U}_{j\mathbf{r}} \right] \hat{U}_{i\mathbf{r}}^{\dagger} \hat{U}_{j\mathbf{r}} + \text{c.c.} ; \quad (5)$$

where \hat{U}^{ij} is the scattering path operator between sites i and j and $\hat{U}_i = \hat{U}_{i\mathbf{r}}^{\dagger} \hat{U}_{i\mathbf{r}}$, with $\hat{U}_{i\mathbf{r}}$ being a single scattering operator for the atom at site i . If not stated otherwise, all the results discussed later would have been obtained with the exchange parameters calculated using Eq. (5).

2. Energy Differences Approach

In this approach the total energies of the TMOs in the ferromagnetic (FM) and antiferromagnetic I and II (AFI and AFII) configurations are taken into account. The AFI structure is characterized by oppositely magnetized planes which are stacked in (100)-direction. Suppose that magnetic interactions operate only between TM atoms | an assumption which is to be discussed later | the mapping onto the Heisenberg Hamiltonian yields

$$J_1 = \frac{1}{16} (E_{\text{AFI}} - E_{\text{FM}}) \quad (6)$$

and

$$J_2 = \frac{1}{48} (4E_{\text{AFII}} - 3E_{\text{AFI}} - E_{\text{FM}}) ; \quad (7)$$

where J_1 describes the interaction between the NN and J_2 that of the next nearest neighbours (see Fig. 1). This mapping also assumes that the interaction between NN is independent of the sublattice the TM atoms are located on. Of course the choice of the three above mentioned structures restricts one to the determination of J_1 and J_2 only. Using more magnetic structures and hence calculating more exchange parameters is in principle possible. However, due to the nature of the present exchange mechanism, the superexchange, this has usually not been done for the TMOs. Although with this method we also restrict exclusively to J_1 and J_2 , it is hoped that the comparison with the MFT method will shed some light on the validity of the underlying assumptions for the TMOs.

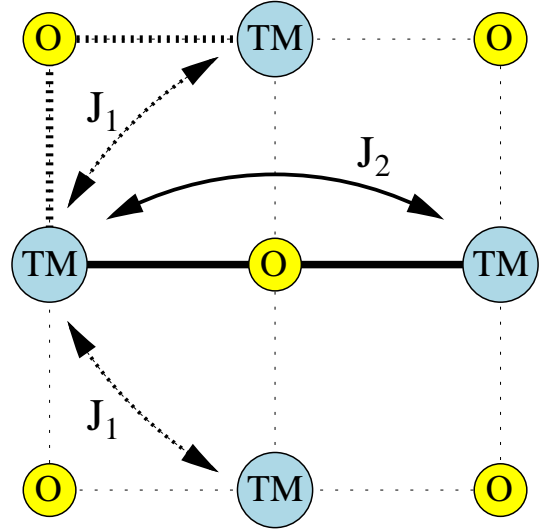


FIG. 1: (color online) Schematic representation of the magnetic interactions in a (100) plane of the rocksalt structure of TMOs. The TM ions (blue) interact via J_1 (dotted arrows) with their nearest and via J_2 (solid arrow) with their next nearest neighbours. In Anderson's super-exchange picture the indirect exchange is mediated by O ions (yellow circles), resulting in a 90° and a 180°-exchange interaction for J_1 and J_2 , respectively. Note that J_1 also contains contributions from direct overlap.

C. Neel Temperatures

Having calculated the exchange parameters for an antiferromagnetic one is able to calculate the Neel temperatures, T_N . Several different approximations can be used, in particular the mean field approximation, the random phase approximation and classical Monte Carlo simulations.

1. Random Phase Approximation

In the RPA one solves the equation of motion for the Green function of the spin operators. Following the approach of Rusz et al.³¹, one ends up with a semi-classical formula for the average spin polarization $\langle \mathbf{S}_i^z \rangle(T)$ of a sublattice (e.g. A), as a function of temperature T ,

$$\langle \mathbf{S}_i^z \rangle(T) = L \left(\frac{2}{k_B T} \right) \frac{1}{N} \sum_{\mathbf{q}} \langle \mathbf{S}_i^z \rangle(\mathbf{q})_{AA} \quad (8)$$

Here $L(x)$ is the Langevin function, $L(x) = \coth(x) - 1/x$, V is the volume of the first Brillouin zone and k_B denotes the Boltzmann constant. The matrix elements of $N(\mathbf{q})$ are defined as

$$N_{AB}(\mathbf{q}) = \sum_C J_{AC}(0) \langle \mathbf{S}_C^z \rangle - \langle \mathbf{S}_A^z \rangle J_{AB}(\mathbf{q}); \quad (9)$$

with the Fourier transforms of the exchange parameters given by

$$J_{AB}(\mathbf{q}) = \frac{1}{N} \sum_{\mathbf{r}} J_{jk} e^{i\mathbf{q} \cdot (\mathbf{R}_j - \mathbf{R}_k)} \delta_{jA} \delta_{kB}; \quad (10)$$

where N denotes the number of interacting magnetic sites and δ_{jA} equals one if site j is on the magnetic sublattice A and zero otherwise. Eq. (8) has to be solved self-consistently since the unknown quantity appears on its left and implicitly also on the right, via $N(\mathbf{q})$. The Neel temperature is equal to the highest value of T at which $\langle \mathbf{S}_i^z \rangle(T)$ becomes different from zero.

2. Mean-Field Approximation

To obtain the MFA estimate of the Neel temperature, a matrix with elements

$$A_{AB} = \frac{2}{3k_B} J_{AB}(0) \quad (11)$$

is constructed^{32,33}, where $J_{AB}(0)$ stands for the Fourier transform of the exchange parameters, defined via Eq. (10), at $\mathbf{q} = 0$. The largest eigenvalue of A yields the Neel temperature. If for any TMO in the AFII structure only the nearest and next-nearest neighbour interactions are considered (J_1 and J_2 , respectively), then the largest eigenvalue yields the well-known relation, $k_B T_N = 4J_2$, indicating that the nearest neighbour interaction J_1 does not have any influence on T_N . Since fluctuations are completely neglected in MFA the resulting Neel temperatures are commonly overestimated.

3. Monte Carlo Simulations

We give a rather brief summary of the method of MC simulations as they are performed in this paper. For a

deeper and complete understanding we refer the reader to the book by Landau and Binder³⁴.

To estimate T_N via MC simulations a lattice representing the structure of the investigated system is constructed. The magnetic moment at lattice site i interacts with its neighbours j via the J_{ij} . During a MC run one picks a lattice site j with the magnetic moment vector \mathbf{e}_j , creates a new random direction \mathbf{e}_j^0 and decides by looking at the energy of the system whether \mathbf{e}_j^0 is accepted or \mathbf{e}_j is kept. Performing this procedure N times on a lattice of N sites is defined as one MC step.

Starting from a certain initial configuration the system is brought into thermal equilibrium for a fixed temperature. After this, "measurements" and thermodynamical averaging of the observables of interest are performed. Since it is impossible during a simulation run to go through all possible configurations of the system, which would be formally necessary for averaging, one must ensure that the configurational subspace that one is restricted to is of physical significance. This is done by performing the so-called importance sampling. It is applied when one has to decide between the old and new magnetic moment vectors \mathbf{e}_j^0 and \mathbf{e}_j described above. There exist several methods to do this, in the present paper the Metropolis algorithm³⁵ is used.

One must be aware of the fact that the finite size of the lattice, despite being periodic in all 3 dimensions, leads to a systematic error in the determination of the critical temperature. This so-called finite-size effect, however, becomes smaller with increasing lattice size. It can therefore be eliminated by extrapolating the critical temperatures for different lattice sizes.

For a magnetic system as in the present case it is straightforward to measure two quantities. One is the staggered magnetization³⁶ m_s being some sort of an average of the absolute values of magnetization of the sublattices,

$$m_s = \frac{1}{N} \sum_{j=1}^N |\mathbf{e}_j \cdot \mathbf{Q}| \quad (12)$$

Here, j labels the lattice sites being N in total, \mathbf{e}_j is the unit vector of the magnetic moment at lattice site j and \mathbf{Q} is the normal vector of the planes of equal magnetization, in the AFII structure being $(1; 1; 1)$ for example. As a note, m_s is used instead of the total magnetization since the latter is equal to zero in antiferromagnets. The other quantity measured is the inner, i.e. magnetic, energy of the system E , which is given by Eq. (4). This whole procedure of relaxing into thermal equilibrium and thermodynamical averaging is repeated for different temperatures. In principle one can determine T_N from the slope of the temperature dependence of $m_s(T)$ and $E(T)$. However, there are quantities that show the critical temperatures more clearly. These are the magnetic susceptibility derived from m_s , the specific heat derived from E , and the 4th-order cumulant³⁷ U_4 . The first two have a singularity at $T = T_N$, the last one has the property that the curves $U_4(T)$ calculated for different lattice sizes

have a crossing point at $T = T_N$.

4. Quantum Effects

As already mentioned, the three approaches described above are based on mapping of the single magnetic moment interactions onto a classical Heisenberg Hamiltonian. These moments, however, are quantum objects and this should in some way be accounted for in the calculations. Wan, Yin and Savrasov³⁸ and Harrison³⁹ did this by replacing the classical S^2 in the Heisenberg Hamiltonian with the quantum mechanical expectation value $S(S+1)$, when calculating magnetic properties. Since in Eq. (4) S^2 is included in the J_{ij} ³⁰, then to be consistent, one has to divide again by S^2 . This gives rise to a factor $(S+1)/S$ for the energy and, eventually, also for the Neel temperature⁴⁰. This factor is, however, not needed when the Neel temperature is obtained based on the DLM method since it does not explicitly use the J_{ij} .

D. Magnon Spectra

With the exchange interactions determined one can also calculate the magnon spectra $E(q)$. They are of special interest since they provide the standard method for determining the exchange parameters experimentally. The latter would be done by fitting a Hamiltonian containing the J_{ij} as fitting parameters to a measured spin wave dispersion. As already mentioned in section II, such Hamiltonians usually contain more terms than the one given in Eq. (4), which is why comparisons between different J_{ij} results must be done carefully.

Considering multiple sublattices one can define magnon spectra as the eigenvalues of the matrix $N(q)$ given by Eq. (9). Assuming two magnetic sublattices, with the same absolute magnetization, and considering only the nearest and next-nearest neighbour interactions, the spectra are given by^{30,41}

$$E(q) = \frac{1}{2} \frac{q^2}{(J_{++}(q) - H_0)^2 - J_+^2(q)} : \quad (13)$$

Here H_0 is the magnetic moment of the two sublattices in units of μ_B , $J_{++}(q)$ ($J_+(q)$) are the Fourier transforms of the intra- (inter-) sublattice exchange parameters expressed respectively as

$$J_{++}(q) = 2J_1 (\cos a(q_x + q_y) + \cos a(q_x - q_y) + \cos a(q_x + q_z)) \quad (14)$$

and

$$J_+(q) = 2J_1 (\cos a(q_x - q_y) + \cos a(q_x - q_z) + \cos a(q_y - q_z)) + 2J_2 (\cos 2a q_x + \cos 2a q_y + \cos 2a q_z); \quad (15)$$

and $H_0 = J_{++}(0) - J_+(0) = 6J_2$. In Eqs. (14) and (15) the vector q and accordingly its components are

needed in units of $2\pi/a$ with a being the lattice constant of the TMO considered.

III. COMPUTATIONAL DETAILS

The transition metal monoxides crystallize in the rock-salt structure (B1, $Fm\bar{3}m$, space group 225). At low temperatures they show small lattice distortions ($< 2\%$). However, these distortions are not considered in the present calculations. The crystal potentials for the ground state calculations are constructed in the atomic sphere approximation (ASA). The ASA radii for the TM and oxygen atoms are chosen as 0.2895 a , with a being the lattice constant of a given TMO. To reduce the ASA overlap while keeping a good space filling, empty spheres are used with the ASA radii equal to 0.1774 a . The ratios of the respective ASA radii are kept constant across the TMO series.

For the electronic structure calculations the complex energy contour has 24 Gaussian quadrature points, and for the Brillouin zone (BZ) integrations a $14 \times 14 \times 14$ k-points mesh is constructed. For the calculation of the magnetic interactions, using the MFT, 60 energy points on a Gaussian mesh in the complex plane are chosen. Convergence of the J_{ij} with respect to the number of k-points is achieved with a $20 \times 20 \times 20$ k-points mesh per energy point for the first 50 of them, and a $60 \times 60 \times 60$ k-mesh for the last 10 energy points, lying close to the Fermi energy. For the MC simulations an fcc-lattice representing the transition metal atoms in the TMO crystal is constructed. To avoid finite-size effects, the size of the lattice is varied from $40 \times 40 \times 40$ to $60 \times 60 \times 60$ elementary fcc cells. To use all observables described in the MC part of Section II one has to restrict the simulations to a relatively small number of MC steps. This is necessary in order to prevent the system from changing the orientation of the ferromagnetic sublattices, for example from (111) to $(\bar{1}\bar{1}\bar{1})$, which are degenerate in energy. Thus, starting from the AF II state, the system is assumed to have reached thermal equilibrium after 5,000 MC steps, and for averaging 10,000 MC steps are performed. If one does so all observables yield the same result for the Neel temperatures for each TMO, respectively. To ensure a thorough exploration of phase space, simulations with up to 100,000 MC steps for averaging have also been performed. In this case the specific heat, not affected by reorientations of the magnetic sublattices, has reassuringly indicated the magnetic phase transitions to occur at the same temperatures as in the short simulations.

IV. RESULTS AND DISCUSSION

A. Exchange parameters

The present calculations of the exchange parameters of TMOs use the ground state electronic structure proper-

ties of these materials as input. The latter are obtained self-consistently with the LSIC method, explained in detail in Ref. 21. In particular, as seen in Eq. (5), for the MFT approach the relevant quantities are the scattering properties evaluated at the equilibrium lattice constant of the ground state, AFII, magnetic structure. For the approach based on the energy differences only the total energies of the FM, AFI and AFII structures, evaluated at the theoretical equilibrium lattice constants of the AFII configuration, are of relevance.

TABLE I: The calculated (calc.) equilibrium lattice constants and spin magnetic moments, per TM-atom, for all the studied TMOs in AFII structure. The oxygen atoms are not spin polarized in the AFII environment and the induced moments on the empty spheres are very small. Consequently the calculated spin magnetic moments of TMOs are practically equal to those of their TM-atoms. The experimental (exp.) values of the magnetic moments contain not only the spin but also orbital contribution.

TMO	a_0 [Å]		μ_B	
	calc.	exp.	calc.	exp.
MnO	4.49	4.44 ⁴²	4.63	4.54 ⁴³
FeO	4.39	4.33 ⁴⁴	3.68	3.32 ⁴⁵
CoO	4.31	4.26 ⁴²	2.69	2.40 ⁴⁶
NiO	4.24	4.17 ⁴²	1.68	1.90 ⁴⁷

From Table I we can see that the LSIC method, treating localized and itinerant electrons on equal footing, reproduces well the equilibrium lattice constants and also the corresponding spin magnetic moments in the AFII structure. The overall agreement with the experimental values is reasonable for both quantities. Note, however, that the experimental magnetic moments listed in the table include both the spin- and orbital-contributions, which are substantial for FeO and CoO, and non-negligible even for NiO. Regarding the calculated spin magnetic moments, they are effectively equal to the spin moments of the TM atoms, as the oxygen atoms are not polarized in the AFII environment, and the induced spin moments on the empty spheres are very small. In addition, as seen in Fig. 2, the spin magnetic moments show considerable dependence on the lattice constants, indicating that a similar behaviour may also be expected for the calculated exchange constants. This dependence of the calculated spin magnetic moments on the lattice constant was also observed in previous studies^{6,15,48} and its trend agrees with the Stoner model, stating that magnetic moments eventually collapse at very high pressures.

Using the above ground state properties in the MFT approach, we have calculated the J_{ij} exchange constants for the first 11 neighbour shells. As expected only the first two of them, J_1 and J_2 , are of relevance as those corresponding to the higher shells are less than 0.1 meV in magnitude. This agrees well with the idea of super-exchange³³ and can easily be explained with it. Consequently, and for the purpose of comparison

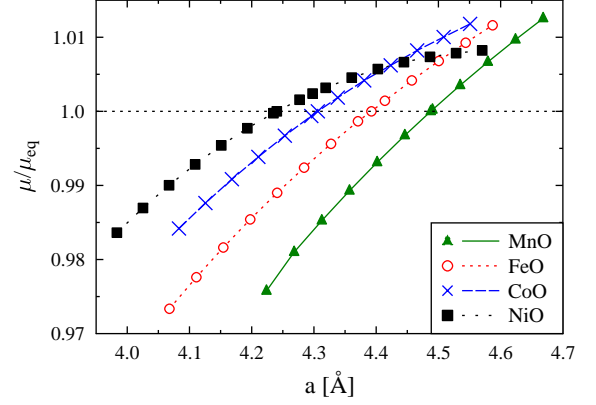


FIG. 2: (color online) The dependence of the calculated spin magnetic moments on lattice constants. The spin magnetic moments have been divided by their respective equilibrium values given in Table I. The crossing points of each curve with the horizontal dotted line at $\mu/\mu_{eq} = 1$ mark the equilibrium lattice constant of each TMO.

with the results of the energy difference approach, in Table II we display only the J_1 and J_2 quantities, as well as the experimental results. Our results also provide justification for one of the assumptions underlying Eqs. (6) and (7), that the interactions between NN atoms are not dependent on the sublattices of the atoms.

From our results in Table II one finds that the J_2 parameters constitute the major part of magnetic exchange in TMOs and that in magnitude they agree reasonably well between the two theoretical approaches, MFT and E. The results are about 70 to 80 % of the experimental values, except for FeO, where the agreement for the MFT J_2 is almost perfect and the E value is larger than the experimental one. This rather accidental agreement for FeO can most likely be attributed to the fact that the experimental values are measured for Wüstite samples $Fe_{1-x}O$ with $x \leq 0.50$. Also, the experimentally observed trend of the increasing absolute value of J_2 across the series is present in both approaches and is most likely associated with the increasing number of the TM 3d electrons, responsible for the magnetic super-exchange. Regarding the quantitative agreement with experiment, the MFT results agree better on average. One could envisage that this agreement could be further improved, if the MFT approach was applied in the DLM state^{29,56}. Nevertheless, compared to the other calculations displayed in Tables II and III, our present results may already be considered as being at least as good as those.

The situation is very different for the J_1 exchange parameters. From Table II we see that, with the exception of NiO, the absolute magnitudes of J_1 are, within about 30%, similar between the two theoretical approaches, but the signs are opposite. Looking more closely at the parameters calculated with the MFT we see that

TABLE II: The exchange parameters, J_i , in meV, with i being the shell index, for the first two shells of all the studied TMOs and both the MFT and E, energy difference, methods. The experimental (exp.) values are given in the leftmost column, respectively, according to the Hamiltanian³⁰ in Eq. (4). For $i > 2$, the absolute magnitudes of the J_i 's for all the TMOs have been less than 0.1 meV. For both the MFT and E approaches the calculated equilibrium lattice constants from Table I have been used. The results of Harrison³⁹, obtained using a tight-binding (TB) formalism for the complete series of TMOs are listed here for a direct comparison. The other previous results, obtained for selected monoxides, are listed in Table III.

TMO	J_1				J_2			
	exp.	MFT	E	TB ³⁹	exp.	MFT	E	TB ³⁹
MnO	-2.06, -2.64 ⁴⁹	-0.91	0.68	-4.41	-2.79 ⁴⁹	-1.99	-1.65	-1.09
FeO	1.04, 1.84 ⁵⁰	-0.65	0.48	-2.99	-3.24 ⁵⁰	-3.17	-3.50	-1.56
CoO	0.70 ⁵¹ , -1.07 ⁵²	-0.32	0.53	-1.83	-6.30 ⁵¹ , -5.31 ⁵²	-4.84	-4.40	-1.64
NiO	-0.69 ⁵³ , 0.69 ⁵⁴	0.15	1.42	-1.44	-8.66 ⁵³ , -9.51 ⁵⁴	-6.92	-6.95	-1.88

TABLE III: Summary of the first principles results for J_1 and J_2 in MnO and NiO, based on the Hamiltanian³⁰ in Eq. (4), from the present and previous theoretical works for comparison. Only those close to experimental values are listed. For details see the corresponding references. We found one result by Feng²³ for CoO, obtained by using the B3LYP hybrid functionals method, $J_1 = 47.12$ meV and $J_2 = 42.56$ meV. To our knowledge no further theoretical papers giving numerical values for the exchange parameters of FeO exist.

MnO			NiO		
method	J_1 [meV]	J_2 [meV]	method	J_1 [meV]	J_2 [meV]
exp.	-2.06, -2.64	-2.79	exp.	-0.69, 0.69	-8.66, -9.51
this work	-0.91	-1.99	this work	0.15	-6.92
LDA + U ⁴¹	-2.50	-6.60	GGA + U ¹⁵	0.87	-9.54
OEP ⁴¹	-2.85	-5.50	SIC-LMTO ²⁰	0.90	-5.50
PBE + U ²²	-2.21	-1.16	Fock35 ⁵⁵	0.95	-9.35
PBE ²²	-3.10	-3.69	B3LYP ⁵⁵	1.20	-13.35
HF ²²	-0.73	-1.16	UHF ⁵⁵	0.40	-2.30
B3LYP ²³	-2.64	-5.52			

the results show the opposite trend to that found for J_2 . Namely, the antiferromagnetic coupling is getting weaker as one moves from MnO to CoO, and in NiO it becomes ferromagnetic. This can be explained by assuming both kinds of interaction to be present and to be competing, in the direct and indirect exchange between NN TM atoms. The picture is relatively intuitive for the direct case. For Mn, which has half filled d-shells, one expects antiferromagnetic coupling since an electron hopping from one Mn atom to the other one keeps its spin. Thus, this transfer clearly prefers antiferromagnetic alignment of the Mn atom⁵⁷. Moving across the TMO series the occupation of the minority spin channels is growing. This increases the probability of an electron hopping, if the TM atoms are ferromagnetically aligned. Thus, the character of the exchange should go towards ferromagnetic, which is what we find for the J_1 calculated via the MFT. Regarding the indirect exchange, we can also follow Goodenough⁵⁷. Nearest TM neighbours interact antiferromagnetically when two electrons in the same oxygen p-or s-orbitals are excited to the empty TM e_g -orbitals. The strength of this kind of interaction can be assumed not to change a lot along the TMO series, since the occupation of both the oxygen p-or s- and the TM e_g -orbitals does not change either. Ferromagnetic

coupling on the other hand is provided by electrons of alike spin that are in different orbitals of the O atom. It is strengthened by a growing occupation of t_{2g} -orbitals because this increases intraatomic exchange. Since the t_{2g} -occupancy is rising when moving across the TMO series from MnO to NiO²¹ one would expect that the magnitude of the ferromagnetic interaction increases while the antiferromagnetic does not. This tendency is clearly present in the MFT values for J_1 in Table II.

Looking at the agreement with experiment not much overlap can be spotted. For the MnO the agreement is satisfactory considering the simplicity of our Hamiltanian. For FeO the sign is opposite. This could be caused by the above mentioned fact that in experiment Wustite samples of the kind $Fe_{1-x}O$ are investigated while our calculations are performed for the ideal FeO system. For CoO and NiO comparison is difficult since experimental values of opposite signs, but similar absolute magnitude have been measured in different experiments. To conclude the comparison of MFT- J_1 and experimental J_1 one can say that the agreement is not as good as for the J_2 . Possible reasons have just been given, but it also seems that the experimental determination of the J_1 is not as accurate as for the J_2 , as can be seen from the variety of numbers obtained for the same compounds. The

lack of agreement between experimental and MFT values for the J_1 may influence the calculations based on those. For the magnon spectra it could be expected that, besides quantitative differences, due to the different signs even qualitative changes of the curves might occur. We shall see later, however, that the latter is not the case. The effect on the calculated Neel temperatures should be small in any case since the energy contributions of the NN in the AF II structure are canceled out.

For the J_1 calculated with the energy difference approach no obvious trends are seen in Table II, and in addition they are positive for all TMOs. For NiO the latter agrees qualitatively with the MFT $-J_1$ and also with previous theoretical results, and the agreement with those by Kodderitzsch et al.²⁰, $J_1 = 0.9$ meV and $J_2 = -5.5$ meV, is also quantitatively rather good. For the other TMOs the sign of J_1 is opposite to the ones calculated with the MFT, and for MnO and CoO they also do not agree with previous theoretical investigations. The totally different behaviour | compared to the MFT-values | can be explained by looking at the electronic ground states of the calculated AFI and FM structures. In both of them the oxygen atoms carry a magnetic moment, which they do not in the AF II structure. This magnetic moment can be assumed to give rise to magnetic interaction with the neighbouring TM atoms (as a matter of fact, applying the MFT to AFI or FM structures yields NN exchange parameters of several meV in magnitude between TM and oxygen atoms). This, however, is in strong contradiction to the assumptions underlying Eqs. (6) and (7), stating that magnetic interaction only occurs between TM atoms. Thus, when using these equations anyway, this "artificially" created magnetic exchange is projected onto the J_1 and J_2 . The reason for the latter quantity being relatively close to its counterpart calculated with the MFT is probably due to the large energy differences between the AF II conformation and the AFI as well as the FM conformation for each of the TMOs. This obviously reduces the error made in Eq. (7).

It should be mentioned that for all calculated pairs of J_1 and J_2 , using SIC-LSDA, the resulting ground state magnetic structure is that of AF II⁵⁸, despite the relatively large spread of the J_1 parameters. Note that the exchange parameters J_1 and J_2 , obtained for the TMO series by applying the MFT approach to the LSDA ground state electronic structure, show no agreement with experiment, except for NiO, which can perhaps be considered as a lucky coincidence. Furthermore, the J 's are longer-ranged, i.e. their character is more metallic. This agrees with the fact that their uncorrected (no SIC) ground states show only very small or no band gaps at all²¹.

Finally, we would like to comment on the variation of the exchange parameters as a function of lattice constants shown in Fig. 3 for all the TMOs. As one can see, the absolute value of J_2 increases with decreasing a . This is in good agreement with the interpretation of the exchange parameters in terms of overlap integrals. The closer the atoms are, the larger the overlap is between the TM d-

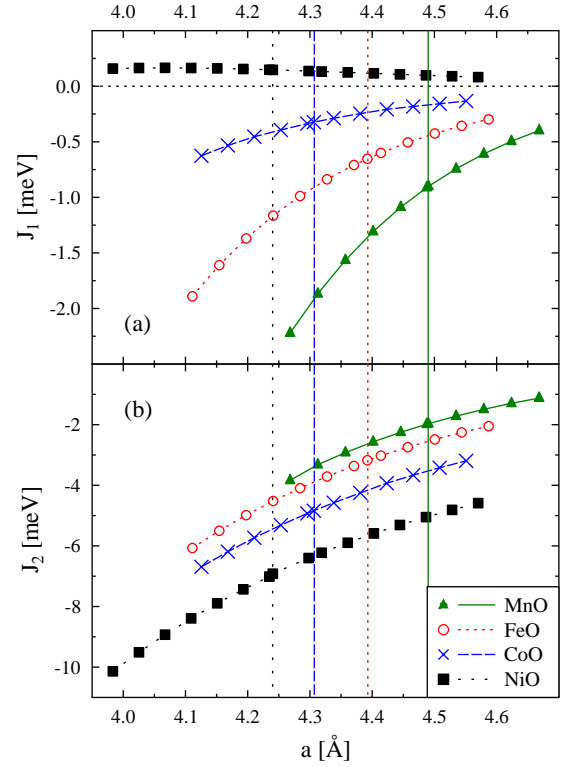


FIG. 3: (color online) (a) The J_1 - and (b) J_2 -dependency on the lattice constant a for all TMOs, calculated using MFT. The vertical lines mark the calculated equilibrium lattice constants from Table I.

orbitals and the oxygen p-orbitals. A similar behaviour is found for the J_1 , which can be understood in the same way as for J_2 . However, going through the TMO series and starting with MnO, the change of the J_1 gets smaller as the antiferromagnetic character becomes less pronounced. According to Goodenough's arguments⁵⁷, this suggests that the ferromagnetic coupling becomes more prominent than the antiferromagnetic one.

B. Neel temperatures

The calculated transition temperatures are summarized in Table IV. One finds that MFA overestimates the experimental Neel temperatures, whereas RPA underestimates them. This is what can be expected from general considerations⁵⁹. One can also see that the Neel temperatures calculated in the RPA approach based only on J_1 and J_2 do not differ significantly from those calculated using the 11 neighbour shells. This again agrees with the idea of superexchange. What is not expected is that, for MnO and FeO the RPA and MC results are relatively small compared to experiment. In fact, for these TMOs the MFA gives a better estimate. The probable reason for that is the general relative underestimate for the J_2 . The latter being the main contribution of mag-

TABLE IV : Summary of the Neel temperatures calculated with the J_{ij} from the MFT approach (see Table II). In the top two rows the experimental and the DLM values are listed, followed by the RPA values based on the interaction of the first 11 TM-TM-shells and of only the nearest and next-nearest neighbours (i.e. only J_1 and J_2). In rows 5 and 6 the MFA results shown, again using 11 or 2 shells, respectively. In the last row the results of the Monte Carlo simulations are presented.

T_N [K]	MnO	FeO	CoO	NiO
Experiment	118	192	289	523
DLM ²⁹	126	172	242	336
RPA with J_{1-11}	81	146	252	440
RPA with $J_{1,2}$	87	155	260	448
MFA with J_{1-11}	122	210	362	628
MFA with $J_{1,2}$	129	221	373	644
MC	90	162	260	458

netic exchange, their underestimate is largest for MnO and decreases towards NiO. An exception is FeO. The agreement for J_2 is almost perfect, yet the RPA and MC estimates are roughly of the same quality as those for the other TMOs. However, it can again (see discussion of J_1 and J_2) be argued that due to the experimental in perfect FeO lattice other effects not considered in our approach may play an important role for the formation of magnetic order. The DLM results of Hughes et al.²⁹ are, with the exception of NiO, in good agreement with the experimental values. Their trend, however, is opposite to ours, namely the ratio $T_N^{\text{DLM}} = T_N^{\text{exp}}$ becomes smaller with increasing atomic number. This could be due to not taking into account the quantum character of the systems, which in the present paper is done via the factor $(S+1) = S^{40}$, where S is calculated according to Hund's rules. Another possible reason especially for the NiO result, as discussed in Ref. 29, might be related to a possible importance of the short range order correlations that a single-site approximation like DLM would not do justice to.

Concentrating on our RPA and MC results, we have to admit that better calculations for the individually selected TMO systems can be found in literature. Among them are the calculations by Zhang et al.¹⁵ for NiO (with a rather semi-empirical approach) and Towler et al.⁶⁰ for MnO. However, when studying the whole TMO series with the same approach, such as the above DLM application, the work reported by Harrison³⁹ or Wan, Yin and Savrasov³⁸, it is hard to find ab initio results, treating electron correlations at the same level of sophistication and predicting the Neel temperatures qualitatively and quantitatively as accurately as in the present paper throughout the whole TMO series.

To finish, we briefly discuss the Neel temperature dependence on pressure shown in Fig. 4 for all the studied TMOs. To calculate the pressure, p , the Mumaghan equation of state⁶¹ has been used. Based on the be-

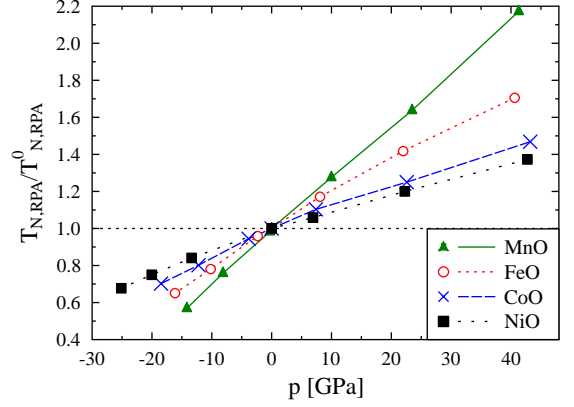


FIG. 4: The normalized RPA-based Neel temperatures $T_{N,RPA} = T_{N,RPA}^0$ for all TMOs as a function of pressure p . $T_{N,RPA}^0$ is taken from row 3 of Table IV.

haviour of J_2 seen in Fig. 3, it is not surprising that for the whole TMO series the calculated Neel temperatures increase with pressure. Qualitatively, this agrees with previous experimental and theoretical results, indicating a stability of the antiferromagnetic structure up to high pressures (several tens of GPa, at least) before it collapses and a paramagnetic or low spin configuration takes over.^{4,6,15,62,63,64,65,66,67,68} We can compare the pressure dependency of T_N to experiment (for MnO { Ref. 4, FeO { Ref. 66, CoO { Ref. 63, NiO { Ref. 65) for $p > 0$ by assuming them to be linear. Taking the pressure derivative of the normalized Neel temperatures, $(\partial T_N / \partial p)_{p=0} = (\partial T_N / \partial p)_{p=0}$, we find that our calculated values increase too slowly, roughly by a factor of 1/2.

C. Magnon Spectra

Considering the above results for the J_{ij} parameters it is reasonable to assume that only the nearest and next-nearest neighbour interactions contribute significantly to the magnon dispersion relation, which therefore should be adequately represented by Eq. (13). For the calculation the MFT- J_1 and J_2 from Table II and the theoretical (calc.) magnetic moment from Table I were used. The resulting magnon spectra for all the studied TMOs, in the AF II structure, are shown in Fig. 5 together with the experimental results. Generally, the agreement between the calculated dispersion curves and the experimental observations is rather good, considering the Heisenberg Hamiltonian used in this work | anisotropy and alignment energy terms are neglected. This is also the reason why the calculated curves fail to reproduce the non-zero energies at $M = (0.5; 0.5; 0.5)$. Besides that, minima, maxima and curvature are well reproduced. Furthermore it can be seen that except for FeO the theoretical curves generally underestimate the experimental energies, which is due to the underestimate of the J_2 parameters. The

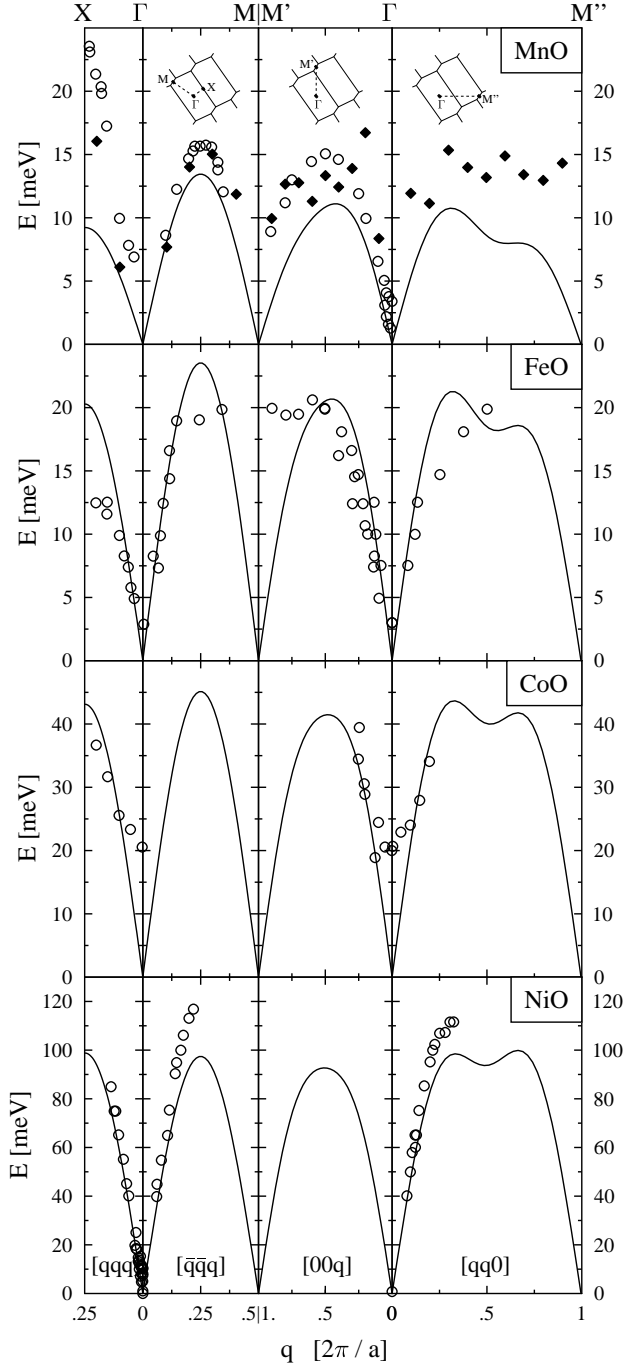


FIG. 5: Shown are the calculated TM O spin wave dispersions together with experimental data points for MnO (black diamonds¹⁰, open circles⁴⁹), FeO⁵⁰, CoO⁵¹ and NiO⁵⁴, respectively. The coordinates are cartesian and in units of $2\pi/a$. The path chosen along several high symmetry lines starts at $X = (0.25; 0.25; 0.25)$ and goes along $[qqq]$ to $\Gamma = (0; 0; 0)$, then along $[q̄qq]$ to $M = (0.5; 0.5; 0.5)$, and further along $[00q]$ to Γ of the neighbouring AF II Brillouin zone, then continuing along $[qq0]$ to M'' . The inlays in the MnO panel show the different branches along the AF II Brillouin zone.

relative magnitude of the peak along $[qqq]$ varies strongly, as one goes through the TM O series. This effect can be ascribed to the changing ratio of $J_2 = J_1$. The qualitative agreement with previous theoretical works, e. g. such as that of Solovyev and Terakura⁴¹ is good, although not in the absolute numerical terms, arising from different values of the Heisenberg exchange parameters J_{ij} .

V. CONCLUSION

We have used the local self-interaction correction, implemented in the multiple scattering theory in the framework of KKR in combination with the magnetic force theorem to study magnetic interactions in transition metal monoxides. Specially, we have calculated the J_1 and J_2 exchange parameters, the corresponding Neel temperatures and the respective magnon spectra for the whole TM O series. The most important conclusion of this work is that the combined approach used here provides an adequate description of magnetic interactions for the series as a whole. Without considering correlation effects the theoretical results in general do not agree with experimental findings. Furthermore, we have shown that our ab-initio approach yields upper (MFA) and lower limits (RPA, MC simulations) for the Neel temperatures for the whole TM O series, and the calculated magnon spectra are in good qualitative agreement with experiment and other theoretical calculations.

Acknowledgements

We would like to thank Julie Staunton for helpful discussions and comments. This work was supported by the Deutsche Forschungsgesellschaft (DFG) via the SFB 762 "Functionality of Oxidic Interfaces". Calculations were performed at the John von Neumann Institute for Computing in Jülich, Germany. Research at the Oak Ridge National Laboratory was sponsored by the Division of Materials Sciences and Engineering, Office of Basic Energy Sciences, US Department of Energy, under Contract DE-AC 05-00OR 22725 with UT-Battelle, LLC.

- ¹ V. V. Struzhkin, H.-K. Mao, J. Hu, M. Schwoerer-Bohning, J. Shu, R. J. Hemley, W. Sturhahn, M. Y. Hu, E. E. Alp, P. Eng, et al., *Phys. Rev. Lett.* **87**, 255501 (2001).
- ² M. Lines and E. Jones, *Phys. Rev.* **139**, A1313 (1965).
- ³ J. R. Patterson, C. M. A. Racine, D. D. Jackson, V. M. Alba, S. T. Weir, P. A. Baker, and Y. K. Vohra, *Phys. Rev. B* **69**, 220101(R) (2004).
- ⁴ C. S. Yoo, B. Maddox, J. H. P. Klepeis, V. Iota, W. Evans, A. McMahon, M. Y. Hu, P. Chow, M. Somayazulu, D. Hausmann, et al., *Physical Review Letters* **94**, 115502 (2005).
- ⁵ A. M. Attila, J.-P. Rue, J. Badro, G. Vanko, and A. Shukla, *Physical Review Letters* **98**, 196404 (2007).
- ⁶ D. K. Asinathan, J. Kunes, K. Koepemik, C. V. Diaconu, R. L. Martin, I. D. Prodan, G. E. Scuseria, N. Spaldin, L. Petit, T. C. Schulthess, et al., *Phys. Rev. B* **74**, 195110 (pages 12) (2006).
- ⁷ U. W. Dowlik and D. Legut, *J. Phys. Chem. Sol.* **69**, 1698 (2008).
- ⁸ A. L. Goodwin, M. G. Tucker, E. R. Cope, M. T. Dove, and D. A. Keen, *Phys. Rev. B* **72**, 214304 (2005).
- ⁹ A. L. Goodwin, M. G. Tucker, M. T. Dove, and D. A. Keen, *Physical Review Letters* **96**, 047209 (pages 4) (2006).
- ¹⁰ A. L. Goodwin, M. T. Dove, M. G. Tucker, and D. A. Keen, *Phys. Rev. B* **75**, 075423 (pages 9) (2007).
- ¹¹ F. Ott, *J. Phys.: Condens. Matter* **20**, 264009 (2008).
- ¹² P. J. van der Zaag, Y. Ijiri, J. A. Borchers, L. F. Feiner, R. M. Wolf, J. M. Gaines, R. W. Erwin, and M. A. Verheijen, *Phys. Rev. Lett.* **84**, 6102 (2000).
- ¹³ O. Bengone, M. Abouani, P. Blochl, and J. Hugel, *Phys. Rev. B* **62**, 16392 (2000).
- ¹⁴ A. Rohrbach, J. Hafner, and G. Kresse, *Phys. Rev. B* **69**, 075413 (2004).
- ¹⁵ W.-B. Zhang, Y.-L. Hu, K.-L. Han, and B.-Y. Tang, *Phys. Rev. B* **74**, 054421 (2006).
- ¹⁶ W. M. Temmerman, A. Svane, Z. Szotek, and H. Winter, in *Electronic Density Functional Theory: Recent Progress and New Directions*, edited by J. F. Dobson, G. Vignale, and M. P. Das (Plenum, New York, 1998), p. 327.
- ¹⁷ W. Temmerman, A. Svane, Z. Szotek, H. Winter, and S. Beiden, in *Electronic Structure and Physical Properties of Solids – The use of the LMTO Method* (Springer, Berlin Heidelberg New York, 2000), Lecture notes in Physics.
- ¹⁸ A. Svane and O. Gunnarsson, *Physical Review Letters* **65**, 1148 (1990).
- ¹⁹ Z. Szotek, W. M. Temmerman, and H. Winter, *Phys. Rev. B* **47**, 4029 (1993).
- ²⁰ D. Kodderitzsch, W. Hergert, W. M. Temmerman, Z. Szotek, A. Ernst, and H. Winter, *Phys. Rev. B* **66**, 064434 (2002).
- ²¹ M. Dane, M. Luders, A. Ernst, D. Kodderitzsch, W. Temmerman, Z. Szotek, and W. Hergert, *Journal of Physics: Condensed Matter* **21**, 045604 (2009).
- ²² C. Franchini, V. Bayer, R. Podbucky, J. Paier, and G. Kresse, *Phys. Rev. B* **72**, 045132 (pages 6) (2005).
- ²³ X. Feng, *Phys. Rev. B* **69**, 155107 (2004).
- ²⁴ J. Kunes, V. I. Anisimov, S. L. Skornyakov, A. V. Lukoyanov, and D. Vollhardt, *Physical Review Letters* **99**, 156404 (2007).
- ²⁵ J. P. Perdew and A. Zunger, *Phys. Rev. B* **23**, 5048 (1981).
- ²⁶ A. Liechtenstein, M. Katsnelson, V. Antropov, and V. Gubanov, *J. of Mag. Mat.* **67**, 65 (1987).
- ²⁷ M. Luders, A. Ernst, M. Dane, Z. Szotek, A. Svane, D. Kodderitzsch, W. Hergert, B. L. Gyor, and W. M. Temmerman, *Phys. Rev. B* **71**, 205109 (2005).
- ²⁸ I. D. Hughes, M. Dane, A. Ernst, W. Hergert, M. Luders, J. Poulter, J. B. Staunton, A. Svane, Z. Szotek, and W. M. Temmerman, *Nature* **446**, 650 (2007).
- ²⁹ I. Hughes, M. Dane, A. Ernst, W. Hergert, M. Luders, J. B. Staunton, Z. Szotek, and W. Temmerman, *New Journal of Physics* **10**, 063010 (2008).
- ³⁰ The Heisenberg Hamiltonian can be defined in several ways. Often the sum is multiplied with the factor 1/2, which corresponds to counting each ij-pair only once. Sometimes the minus sign is omitted. In our case also the absolute values of the spin vectors S_i and S_j are included in the J_{ij} and instead the unit vectors e_i and e_j are used. One has to take care of this when comparing exchange parameters J_{ij} of different works.
- ³¹ J. Rusz, I. Turek, and M. Davis, *Phys. Rev. B* **71**, 174408 (2005).
- ³² E. Sasioglu, L. M. Sandratskii, and P. Bruno, *Phys. Rev. B* **70**, 024427 (2004).
- ³³ P. W. Anderson, *Theory of Magnetic Exchange Interactions: Exchange in Insulators and Semiconductors*, vol. 14 of *Solid State Physics* (Academic Press, New York, 1963).
- ³⁴ D. Landau and K. Binder, *A Guide to Monte Carlo Simulations in Statistical Physics* (Cambridge University Press, 2000).
- ³⁵ N. Metropolis, A. Rosenbluth, M. Rosenbluth, A. Teller, and E. Teller, *J. Chem. Phys.* **21**, 1087 (1953).
- ³⁶ W. Xue, G. S. Grest, M. H. Cohen, S. K. Sinha, and C. Soukoulis, *Phys. Rev. B* **38**, 6868 (1988).
- ³⁷ K. Binder, *Z. Phys. E* **43**, 361 (1981).
- ³⁸ X. Wan, Q. Yin, and S. Y. Savrasov, *Phys. Rev. Lett.* **97**, 266403 (2006).
- ³⁹ W. A. Harrison, *Phys. Rev. B* **76**, 054417 (2007).
- ⁴⁰ For the MC simulations this factor for the Hamiltonian corresponds to a scaling of the temperature with the same factor. A quantum mechanical calculation for the MFA yields³³ $\chi_{AB} = \frac{2}{3k_B} \frac{(S+1)}{S} J^{AB}(0)$ for the TMO. So going from classical to quantum treatment also corresponds to multiplying with $(S+1)/S$. Therefore, we multiplied the classical RPA result with $(S+1)/S$, analogous to the MFA. The values obtained from this show excellent agreement with such we get by using the RPA approach by Lines⁶⁹, which is a quantum approach that, however, considers only nearest and next-nearest neighbour interaction and is valid only for the TMO and materials with the same magnetic structure.
- ⁴¹ I. V. Solov'ev and K. Terakura, *Phys. Rev. B* **58**, 15496 (1998).
- ⁴² G. I. Landolt-Bornstein, *New Series, Numerical Data and Functional Relations in Science and Technology*, vol. 27g, Various Oxides (Springer Verlag, 1992).
- ⁴³ W. Jauch and M. Reehuis, *Phys. Rev. B* **67**, 184420 (2003).
- ⁴⁴ H. Fjellvåg, F. Gronvold, S. Stolen, and B. Hauback, *Journal of Solid State Chemistry* **124**, 52 (1996).
- ⁴⁵ W. L. Roth, *Phys. Rev.* **110**, 1333 (1958).
- ⁴⁶ W. Jauch and M. Reehuis, *Phys. Rev. B* **65**, 125111 (2002).
- ⁴⁷ A. K. Cheetham and D. A. O. Hope, *Phys. Rev. B* **27**, 6964 (1983).

- ⁴⁸ Z. Fang, I. V. Solov'yev, H. Sawada, and K. Terakura, *Phys. Rev. B* **59**, 762 (1999).
- ⁴⁹ G. Peppy, *J. Phys. Chem. Sol.* **35** (1974), 47.
- ⁵⁰ G. E. Kugel, B. Hennion, and C. Carabatos, *Phys. Rev. B* **18**, 1317 (1978).
- ⁵¹ K. Tomiyasu and S. Itoh, *J. Phys. Soc. Jpn.* **75**, 084708 (2006), 43.
- ⁵² M. D. Rechten and B. L. Averbach, *Phys. Rev. B* **6**, 4294 (1972).
- ⁵³ R. Shanker and R. A. Singh, *Phys. Rev. B* **7**, 5000 (1973).
- ⁵⁴ M. Hutchings and E. Samuelson, *Phys. Rev. B* **6**, 3447 (1972).
- ⁵⁵ I. P. R. Moreira, F. Illas, and R. L. Martin, *Phys. Rev. B* **65**, 155102 (2002).
- ⁵⁶ S. Shallcross, A. E. Kiskavos, V. Meded, and A. V. Ruban, *Phys. Rev. B* **72**, 104437 (2005).
- ⁵⁷ J. B. Goodenough, *Magnetism and the Chemical Bond* (Interscience, New York, 1963).
- ⁵⁸ M. S. Seehra and T. M. Giebultowicz, *Phys. Rev. B* **38**, 11898 (1988).
- ⁵⁹ J. Rusz, I. Turek, and M. Davis, *Phys. Rev. B* **71**, 174408 (2005).
- ⁶⁰ M. D. Towler, N. L. Allan, N. M. Harrison, V. R. Saunders, W. C. Mackrodt, and E. Apra, *Phys. Rev. B* **50**, 5041 (1994).
- ⁶¹ F. D. Mumaghan, *Proc Natl Acad Sci U S A* **30**, 244 (1944).
- ⁶² Y. Ding, Y. Ren, P. Chow, J. Zhang, S. C. Vogel, B. Winkler, J. Xu, Y. Zhao, and H. K. Mao, *Phys. Rev. B* **74**, 144101 (pages 4) (2006).
- ⁶³ W. B. Holzapfel and H. G. Drickamer, *Phys. Rev.* **184**, 323 (1969).
- ⁶⁴ D. Bloch, F. Chaisse, and R. Pauthenet, *Journal of Applied Physics* **37**, 1401 (1966).
- ⁶⁵ V. A. Sidorov, *Applied Physics Letters* **72**, 2174 (1998).
- ⁶⁶ T. Okamoto, H. Fujii, Y. Hidaka, and E. Tatumoto, *Journal of the Physical Society of Japan* **23**, 1174 (1967).
- ⁶⁷ D. G. Isaak, R. E. Cohen, M. J. Mehl, and D. J. Singh, *Phys. Rev. B* **47**, 7720 (1993).
- ⁶⁸ J. Badro, V. V. Struzhkin, J. Shu, R. J. Hemley, H.-k. Mao, C.-C. Kao, J.-P. Rue, and G. Shen, *Physical Review Letters* **83**, 4101 (1999).
- ⁶⁹ M. Lines, *Phys. Rev.* **135**, A1336 (1964).